Sensors and Actuators A 219 (2014) 73–79

Contents lists available at ScienceDirect

Sensors and Actuators A: Physical

journal homepage: www.elsevier.com/locate/sna

An electromagnetic energy harvesting device based on high efficiency windmill structure for wireless forest fire monitoring application

Xuan Wu, Dong-Weon Lee*

MEMS and Nanotechnology Laboratory, School of Mechanical Engineering, Chonnam National University, Gwangju 500757, South Korea

ARTICLE INFO

Article history:
Received 24 June 2014
Received in revised form 6 August 2014
Accepted 2 September 2014
Available online 16 September 2014

Keywords:
Energy harvesting
Electromagnetic
Windmill structure
Forest fire
Wireless sensors network

ABSTRACT

In this paper, we introduce a miniature windmill-structured energy harvester for wireless monitoring of forest fires. The proposed energy harvester design can effectively scavenge the energy from ambient air flow using electromagnetism, thereby self-powering the wireless sensing nodes for fire alarming. To find an optimal structure with the highest aerodynamic efficiency and sensitivity to wind flow, miniature energy harvesters with various windmill structures were designed, simulated, 3D printed and experimentally characterized. In the performance test, with the optimized windmill structure, a peak output voltage of 5.2 V and a peak output power of 60 mW were achieved by the energy harvester with a load resistance of 150 Ω. Moreover, a wireless transmission module was designed and connected to the windmill-structured energy harvester to constitute a wireless fire monitoring system. This module successfully transmitted an alarm signal upon detection of a fire in the feasibility test.

1. Introduction

Forest fires, also known as wildfires, are uncontrolled fires occurring in the countryside or wilderness, which result in enormous damage to natural and human resources [1,2]. Wildfires eradicate forests, destroy the ecosystem, and may lead to severe casualties if they are not extinguished timely. The damage caused by accidental wildfires to public safety and natural resources is tremendous and intolerable. For instance, in the United States, typically 40,000–250,000 wildfires occur each year, burning 3 million to 10 million acres of land depending on the year [3]. The black forest fire, which happened in Colorado, June 2013, destroyed 509 homes, and forced the evacuation of 38,000 residents. The estimates of damage are expected to exceed $90 million [4]. Due to dry conditions, high heat and restless winds, fast-spreading forest fires can easily become devastating disasters to the human beings nearby. Therefore, the early detection and suppression of fires are crucial for minimizing the damage and casualties.

Considering the fast-spread characteristic of a forest fire, real-time surveillance of the forest area is desired to minimize the range of the danger zone. Moreover, owing to the vast area of a forest, conventional sensor networks with long-wire bundles incur a huge installation and long-term maintenance cost, limiting the number of sensors that can be installed and thereby reducing the overall quality and reliability of the real-time data reported [5]. For these reasons, the wireless sensors network (WSN) is an appropriate choice for solving these problems. Regarded as one of the most significant technologies in the 21st century, WSNs can realize continuous detection and information monitoring [6,7]. Unfortunately, the battery is one of the most common means to power a widely spread wireless sensor installed in a commercial WSN [8]. Its limited electrical power will result in a high maintenance cost [9]. Moreover, the energy-saving strategy employed in the power management module of each node will reduce the sampling rate and the signal transmission rate as well as the accuracy of the real-time data [10]. To solve these problems, researchers have carried out extensive studies on various energy harvesters to substitute the batteries used in WSN applications [11,12].

Energy harvesters are used to convert the ambient energy into electricity to power small autonomous sensors [13]. Many types of energy sources are available for energy harvesting, such as solar, hydraulic, vibration and wind [14–17]. However, vibration is not available in the forest environment. And, due to the shading by the lush leaves on the trees in a forest, it is difficult to harvest sufficient solar energy in the forest; furthermore, a large solar panel will have various installation constraints. On the other hand, wind energy, except that from natural wind in normal conditions, would be viable even in a forest fire condition because of the large amounts of air convections that exist during a forest fire from the temperature difference between the fire zone and its surroundings. Based

* Corresponding author. Tel.: +82 62 530 1684; fax: +82 62 530 1689.
E-mail address: mems@jnu.ac.kr (D.-W. Lee).

http://dx.doi.org/10.1016/j.sna.2014.09.002
0924-4247/

on the above considerations, wind is a more effective and reliable source of energy for this application. Therefore, considering the abundance of natural wind and air convection in a forest environment, the use of wind flow as the energy source for the energy harvesting system is reasonable.

Most conventional energy harvesters use piezoelectric materials for power generation [18]. For instance, Bibo et al. [19] proposed a concurrent piezoelectric energy harvester for both ambient wind power and vibrations. Li et al. [20] reported a polymer piezoelectric energy harvester for low-speed wind. However, the high resistances (~kΩ/MΩ or even more) of piezoelectric materials result in very low output currents and powers, which cannot satisfy the minimum power requirement of a small sensor [21]. On the contrary, the electromagnetic method, having low internal resistance (~Ω), can realize much higher output currents and powers than piezoelectric methods [22]. For example,Tang et al. [23] developed a wide frequency-range energy harvester using non-contact, magnetic repulsive-force excitation based on electromagnetism, which can generate a peak power of 4.42 mW (much more than that based on piezoelectric materials, normally only ~μW). Galchev et al. [24] also presented a micro electromagnetic energy harvesting device for low-frequency and nonperiodic vibrations. Therefore, in order to provide high output currents and powers for the sensor nodes in the practical application, the electromagnetic method is utilized in our design.

In this paper, we proposed a unique windmill-structured electromagnetic energy harvester that can convert ambient wind energy into electricity to supply high output current and power for sensing and signal transmission in forest fire monitoring application. Different blades were designed and manufactured utilizing 3D printing technology. A finite element method (FEM) simulation was conducted to determine the blade design with the highest efficiency. Based on this design, a miniature energy harvester prototype was successfully fabricated and experimentally characterized. A preliminary forest fire wireless monitoring system was also realized and demonstrated.

2. Design and modeling

In a forest environment, natural wind is one of the most reliable and sufficient sources of energy. Moreover, once a forest fire occurs, due to the air temperature difference between the fire spot and the area nearby, a large amount of air convection occurs around the fire area [25]. Both of these types of air flow can be utilized by the energy harvester to generate power. Therefore, the design of the energy harvester should be wind-sensitive and should effectively convert wind energy into electricity. A windmill is a machine that converts the energy of wind into rotational energy by means of blades/vanes. This kind of structure can effectively scavenge the wind energy with low noise and high reliability during its long service life. Therefore, we apply the windmill structure to our harvester design to collect the wind energy.

Schematically shown in Fig. 1, a windmill structure is mounted on a frame with a highly lubricated axis. The streamlined frame can selectively allow the wind to pass through the energy harvester in a particular area, as well as reduce the resistance of the wind input. Four identical magnets, protected by the frame, are attached to the ends of the blade in the same pole arrangement, respectively. A copper coil is installed on the frame just below the magnets. When the airflow produced by the environment passes through the windmill-structured energy harvester, the airflow force pushes the blades to rotate about the pivoting axis. Thereby, the alternate magnet-and-no magnet passing condition over the coils will vary the magnetic flux through the loop of copper coils. In this way, according to Faraday's law of induction, electrical energy will be generated when this energy harvester is placed in a wind field [26].

However, the aerodynamic profiles of blades have a crucial influence on the rotating efficiency of the whole windmill structure [27]. Therefore, aiming for high aerodynamic efficiency, 7 types of windmill structures with various types of blades are designed, shown in Fig. 1. The characteristics of these blades are listed in Table 1. It should be noted that compared with the curvature of the type 2 blade, that of the type 3 blade is expected to concentrate the wind more on the blade end to produce a higher rotating moment. The type 4 blade is designed with a concave/convex angle to produce a high rotating torque. The convex side of the blade features pores/indentations can break up the even airflow pattern on the surface. A layer of air will be created directly over the blade surface of this side, which can reduce the resistance and friction as the blade moves through the air [28]. The dimple patterns will increase the strength of the blade. The parallel arranged slots capture and channel the air flow. The slots near the center axis are wider and deeper than those near the outer edge of the blade. The air flow is guided to the blade end and hence, the moment of rotation is enhanced. Type 5 combines the end-concentrated circular arc shape with pores and slots. In type 6, the direction of the slots is changed, which means that the slots near center axis are narrower and shallower than those near the outer edge of the blade. To determine which structure can reduce resistance more during blade rotation, we replace the pores with half spheres on the convex side of the blade surface in the type 7 design.

The number of blade also affects to the performance of the energy harvester. Considering the inherent torque ripple existed in the blades, which influences to the fatigue life of the device as well as the output power quality, three or more blades in the windmill structure are desirable to reduce the torque ripple [29]. In addition, proper number of blades is another important issue to keep a high performance of the energy harvester. In order to avoid the decrease in power generation ability caused by the counteraction of magnetic flux between permanent magnets, a certain distance should be ensured between each magnet in the windmill structure. This leads a limited number of blades as less than five in the present dimension. Based on above considerations, four blades are adopted for each type of windmill structures.

To determine the windmill structure with the highest efficiency, the FEM model of the windmill-structured energy harvester, as well as these 7 types of blades, were built by software COMSOL Multiphysics 4.2. Under same initial conditions, the wind velocity distribution and pressure distribution for each blade working in the energy harvester were simulated respectively. Additionally, the condition of the windmill structure during a rotating cycle was studied by simulating the windmill structure at various angles (0°, 30°, 60°) in a wind field. The insets of Fig. 2(a) and (b) show the simulation results of type 4 for illustration. The inlet wind flowed from the right to the left at 1 m/s.

As shown in Fig. 2(a) and (b), due to the different blade curve shapes – planar shape (type 1), standard circular arc shape (types 2 and 4) and end-concentrated circular arc shape (types 3, 5, 6 and 7), the distributions of wind velocities and pressures of the 7 type of blades presented various characteristics even at same rotating angle. Among the 7 types, type 4 produced the highest wind velocity and maximum pressure at different rotating angles, which meant that it can produce the largest pushing force and highest acceleration during rotation. In this case, with the same input wind velocity and actuation time, type 4 can generate a higher rotating frequency, making it the most efficient blade design. To further confirm the aerodynamic efficiencies of the 7 designs, the performances of the 7 types of blades were characterized by experimental method.

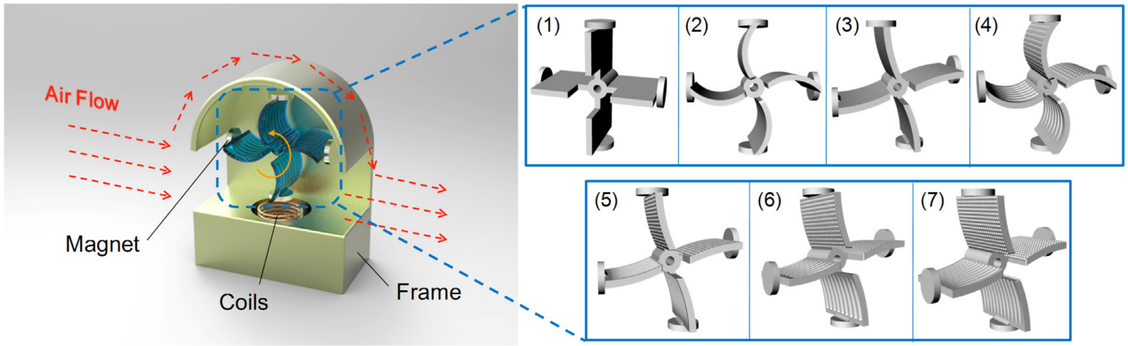

Fig. 1. The working schematic of the windmill-structured energy harvester with various designs of the replaceable windmill structure.

Table 1
Parameters of the seven designed wind blades.

Name	Characteristics of blades	Descriptions
Type 1	Planar shape	Conventional shape
Type 2	Symmetrical circular arc shape	To increase windward area
Type 3	End-concentrated circular arc shape	To make the wind concentrate more on the blade end
Type 4	Standard circular arc shape with pores and slots	Pores: reduce resistance Slots: guide wind
Type 5	End-concentrated circular arc shape with pores and slots	Pores: reduce resistance Slots: guide wind
Type 6	Same as type 5 except the opposite direction of slots	Pores: reduce resistance Slots: guide wind
Type 7	Same as type 5, but the pores are replaced by half spheres with same volume	Half spheres: reduce the resistance Slots: guide wind

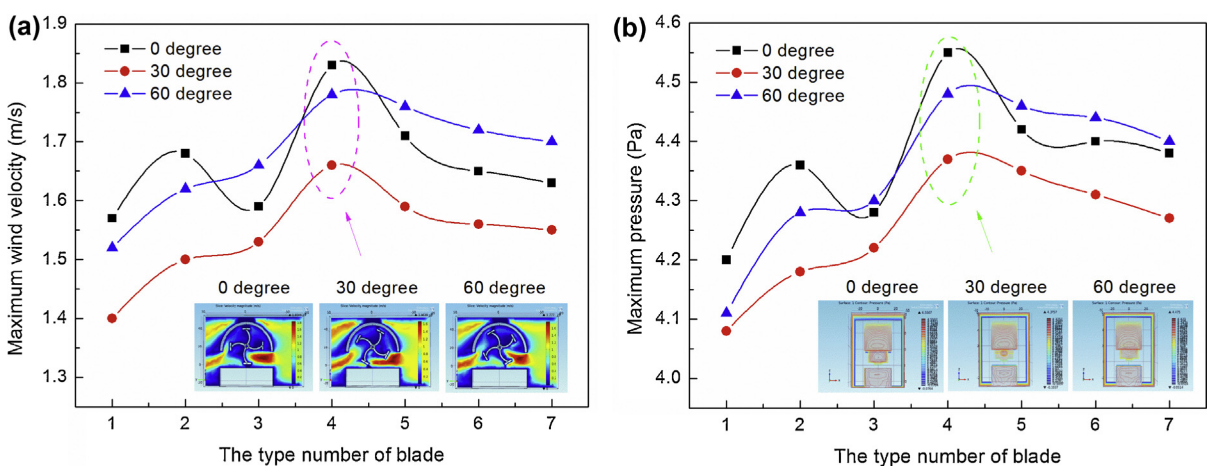

Fig. 2. COMSOL simulation results on the (a) wind velocity distribution and (b) pressure distribution for different types of blades. The input wind velocity is 1 m/s, and the blade is rotating at angles 0°, 30°, 60°, respectively.

3. Fabrication and experiment setup

To realize the core part of the design, various windmill structures were manufactured by 3D printing technology. The complicated surface structures (such as the tiny pores and half spheres) and streamlined blades with slots were expediently realized through the unique additive 3D manufacturing process. This technology also dramatically reduced the fabricating cost compared with traditional machining techniques (subtractive processes) that mostly rely on the removal of material by drilling, cutting, etc. [30]. The material used for the 3D printing technology was Poly(methyl methacrylate) (PMMA). The 7 types of windmill structures could be replaced conveniently in the same 3D printed PMMA frame for more performance – comparison experiments. Additionally, four identical Neodymium–Iron–Boron (NdFeB) magnets were fixed on the blade-ends of the windmill structure in the same magnetic pole arrangement, respectively. Through a highly lubricated ball bearing, the windmill-structure was mounted on the PMMA frame. Under the windmill-structure, a copper coil was mounted in the frame. Since the number of coil turns was restricted by the volume constraint, we chose 3000 as the maximum number of coil turns. The resultant resistance of the coil was 142 Ω, which was measured by a Keithley 2400 source meter (Keithley Instruments, Inc., USA). The details about the geometric dimensions and materials of the fabricated energy harvester are listed in Table S1 (in Supplementary materials).

The experimental setup for the performance testing of the energy harvester is shown in Fig. 3. The wind condition was simulated by placing a DC speed-controlled electric fan in front of the miniature windmill-structured energy harvester. The wind velocity could be adjusted by varying the input DC voltage, which was provided by an Agilent E3642A DC power supply (Agilent

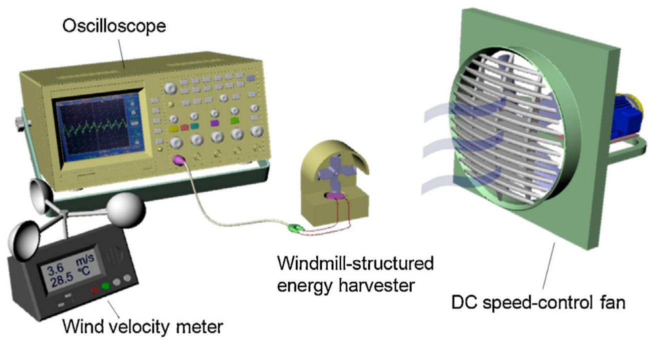

Fig. 3. The schematic of performance test setup.

Technologies, Inc., USA). A Testo 410-1 anemograph (Testo, Inc., Germany) was mounted to measure the wind velocity applied to the energy harvester. According to the Beaufort Wind Scale, the natural wind in daily life usually flows at less than 18 m/s [31]. Therefore, we selected this wind velocity as the maximum input in our experiment. The corresponding wind velocities and land conditions with different Beaufort numbers are listed in Table S2 (in Supplementary materials). By adjusting the input wind velocity, wind velocities in the range of 0–18 m/s could be realized in the performance testing experiment. The output voltage and power generation frequency was measured by a Tektronix TDS 2014B oscilloscope (Tektronix, Inc., USA), which was connected to the energy harvester. These apparatuses were mounted on a vibration isolation table (DVIO-I-2010M-200t, Daeil Systems, Inc., South Korea), which can reduce the interference from the environment.

4. Experimental results and discussion

4.1. Performance testing of various windmill structures

Since the various curvatures of the blades will result in different rotating aerodynamic efficiencies, the 7 windmill structure designs were evaluated for their performances to select the windmill structure with the highest rotating efficiency, which will be used in a real application. For characterizing the rotating efficiency of the windmill structure, two key factors were measured and compared: maximum voltage generation ability and acceleration time. The maximum voltage generation ability decides the maximum operating voltage of the sensing and wireless transmission module that is connected to our design in practical applications. The acceleration time represents the reaction speed of the windmill structure when exposed to a random wind.

According to Faraday's law of induction, the rotating frequency corresponds to the changing rate of the magnetic flux through the loop of the copper coils, which is proportional to the output voltage. Hence, at the same wind velocity, the blade which has the fastest rotating speed/frequency among the 7 types represents the one with the highest voltage generation ability. Therefore, to confirm the maximum voltage generation ability of the designed blades, the rotating frequency of the windmill structure was characterized. With various input wind velocities, the maximum rotating frequency of each windmill structure were measured by the oscilloscope, as shown in Fig. 4(a). Type 4 windmill structure possessed a highest rotating frequency among the 7 designs in the wind velocity range of 0–18 m/s. Moreover, a peak output voltage of 5.6 V was achieved at the maximum rotating frequency with a wind velocity of 18 m/s in the open circuit. This is attributed to the slot and pore structures on the surface of the blade, which largely reduce air friction during blade rotation.

Note that the windmill structures with the standard circular arc shape (types 2 and 4) showed a higher frequency increasing trend than those of the end-concentrated circular arc shape (types 3, 5, 6 and 7) and the planar shape (type 1) in the wind velocity range of 0–12 m/s. Conversely, the windmill structures with the end-concentrated circular arc shape showed higher frequency increasing ability when the wind velocity was above 12 m/s. Moreover, type 5 is expected to have a higher maximum rotating frequency than type 4 when the wind velocity is over 18 m/s. This behavior indicates that the standard circular arc shape is more suitable for achieving high maximum rotating frequency (corresponding to high output voltage) at a low wind speed. Considering the fact that low-velocity wind is much more abundantly available in a forest, type 4 is the most suitable design for our energy harvester in real application. The performances of the 7 windmill structures also confirmed the previous simulation results.

Apart from the voltage generation ability, the acceleration time is also one of the core performance properties of a windmill-structured energy harvester. It reflects the reaction speed and energy scavenging ability of this device under random wind flow, especially under unsteady wind flow. For this reason, the response time to maximum voltage of the windmill-structured energy harvester was measured for various input wind velocities. As Fig. 4(b) shows, type 4 had a lowest acceleration time to reach to maximum output voltage. Its surface structures promoted lower rotating resistance and higher sensitivity of the device to natural unsteady wind than those of the other types.

Therefore, based on the above simulation and experimental results, the type 4 windmill structure had the highest rotating frequency, which was utilized in our subsequent experiments.

4.2. Resistance optimization and output power testing

According to Jacobi's law, maximum power is transmitted when the load impedance is equivalent to the output impedance of the system [32]. In order to transfer the maximum output power, impedance matching is quite important. Hence, load resistance was optimized for the energy harvester. As shown in Fig. 5(a), at various input wind velocities, the maximum output voltage was measured for different load resistances. As the load resistance increased, the output voltage also increased. In this experiment, a peak output voltage of 5.2 V could be achieved with a 2000 Ω resistance under 18 m/s wind velocity. In addition to the peak output voltage, the electrical power from the windmill-structured energy harvester was tested at different load resistances, as shown in Fig. 5(b). It can be observed that the maximum electrical power of 60 mW was generated from the energy harvester at the load resistance value of 150 Ω, fully satisfying the minimum power requirement of a small wireless sensor [33].

Since signal transmission in WSN is intermittent at a certain rate, the energy generated by energy harvester could be stored in a storage circuit and discharged during the signal transmission [34]. In addition, an effective output power is desired for the operated device like the wireless transmission module in different conditions. For these reasons, the average power (root mean square power) under various input wind velocities was investigated. As shown in Fig. 6, based on the above load resistance optimization, the average power generated was measured and calculated for different input wind velocities. The average power at wind speeds in the range from 0 m/s to 18 m/s tended to increase. This is due to the fact that a higher rotating frequency leads to a higher power generating frequency, which results in more power generation. In this experiment, an average power of 3 mW was achieved at the wind velocity of 3 m/s, which contents the minimum average power consumption for a diminutive wireless sensor [35]. The output waveform of the energy harvester is also shown in Fig. 6. Compared with the damping waveforms of conventional designs based on piezoelectric materials, the output waveform can yield higher power, also

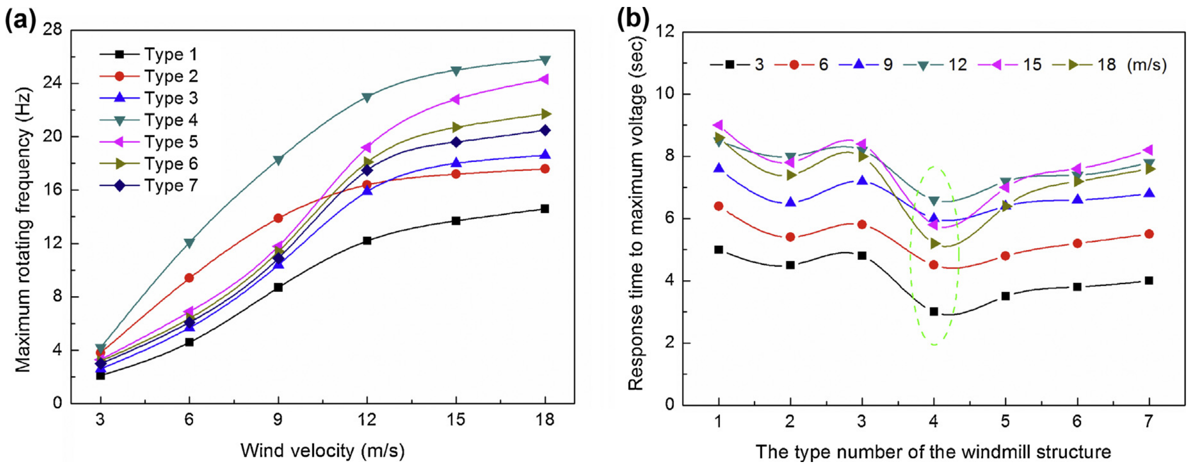

Fig. 4. The performance characterization for the 7 types of windmill structures. (a) The maximum rotating frequency versus input wind velocity. (b) The response time to maximum voltage under various input wind velocities.

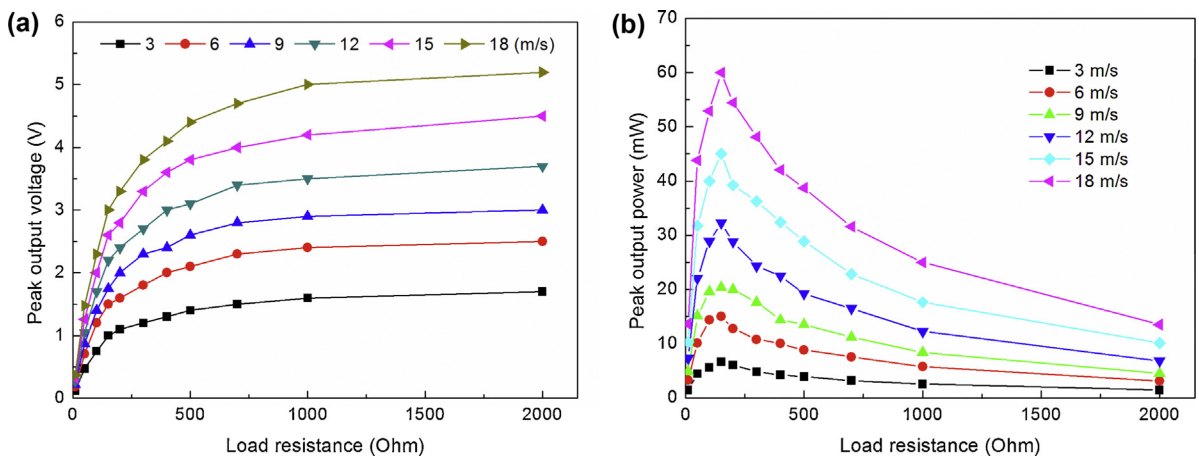

Fig. 5. Resistance optimization: (a) Peak output voltage versus load resistance for different input wind velocities. (b) Peak output power versus load resistance for different input wind velocities.

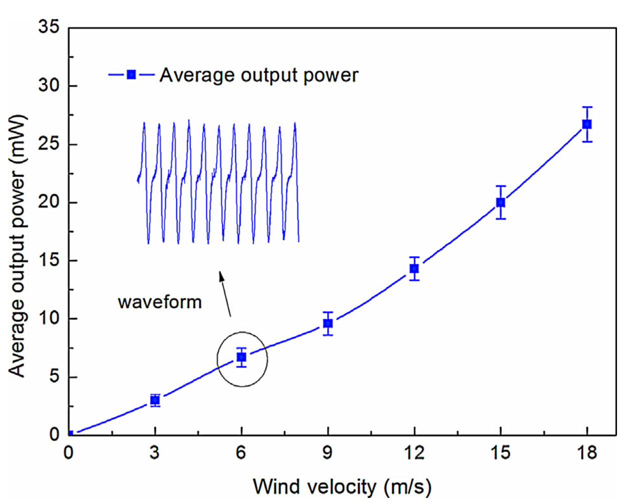

Fig. 6. The average output power of the windmill-structured energy harvester with various input wind velocities.

confirming the experiment results in this study. Moreover, as shown in Fig. S1 (in Supplementary materials), with a minimum wind velocity of 3 m/s, this optimized wind energy harvester could light up a 1.2 V LED.

4.3. Feasibility experiment of wireless monitoring the fire

To demonstrate the concept of a real fire monitoring, a wireless sensing and transmission system based on the windmill-structured energy harvester was characterized using an experimental setup as shown in Fig. 7(a). In the system, a temperature switch sensor (40R0618 Hanguk Electron, Co., Ltd., South Korea) was employed to detect the fire by sensing the heated air flow around a fire. It plays a role of "bridge" between the windmill-structured energy harvester and the wireless transmission module. The temperature sensor has an open circuit configuration in a normal condition. At a temperature over 40 °C (with a fire approach), the temperature switch was closed and the "bridge" became connected. In this case, with adequate nature wind or fire-caused air convection, the windmill-structured energy harvester transfer a power to the wireless transmission module, thereby emitting an alarming signal to the receiver. The alarm LED on the wireless receiver was lighted once the signal was received. On the other hand, for a normal condition (without fire), the "bridge" automatically recovered to disconnection. Consequently, since the energy harvester cannot provide power for the wireless transmission module on this occasion, there was no alarming signal emitted even with sufficient wind flow. In this way, the fire can be effectively detected and alarmed by this system. The detailed circuit diagram of the system is shown in Fig. S2 in Supplementary materials. Furthermore, a super capacitor can be adapted to the proposed system for

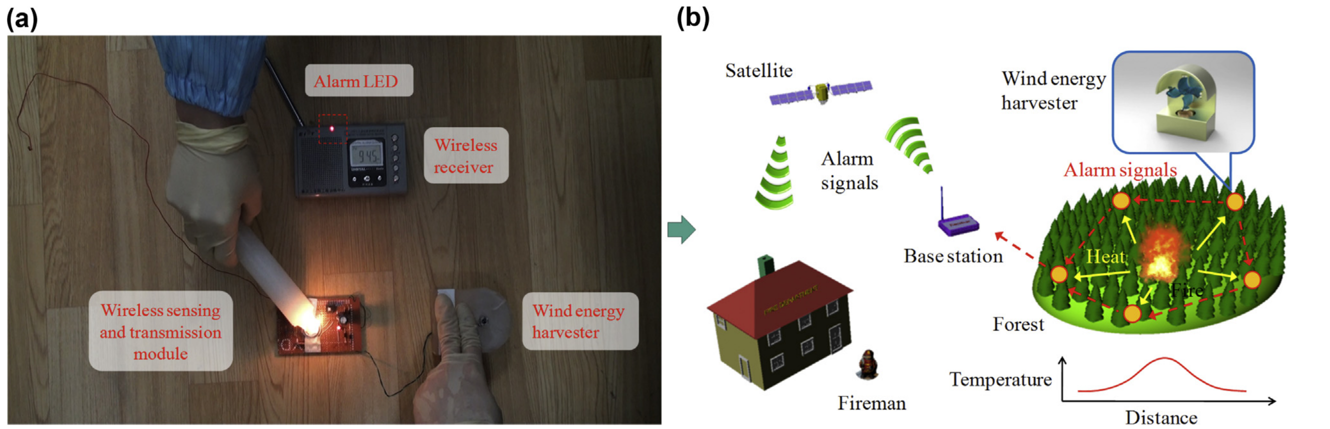

Fig. 7. (a) The experimental setup for windmill-structured energy harvester based fire monitoring and alarming system. (b) The schematic of wireless forest fire monitoring by the windmill-structured energy harvester.

further enhancement in practical applications. This accumulates more power for signal transmission when the energy harvester confronts a low velocity wind flow. Additionally, the wireless transmission module can be improved by using a processor and Zigbee as a radio frequency (RF) device. The advanced module with a DC voltage source of 3.3 V achieves a long distance signal transmission up to 1000 m, which is expected to be realized by our device with a power management module [36].

For real forest fire monitoring as shown in Fig. 7(b), each energy harvester based node combines the temperature switch sensor and the wireless transmission module. Once the forest fire occurs, data is collected at each node around the fire and transmitted to the base station (often names "gateway") directly or indirectly. The indirect transmission of data is realized by using a networking algorithm because these nodes can communicate with each other. Subsequently, the signal which contains the fire position information will be transmitted from base station to the fire department by the Global Positioning System (GPS). According to the alarming signal, the fire patrol can easily locate the fire point in the extensive forest [37].

Based on the above working principle, the sensing area of each node is quite significant for this application, which will directly decide the quantity of utilized nodes in this network and the total cost. For this reason, a fire temperature distribution analysis around a forest fire is conducted (see in Fig. S3 in Supplementary materials). When a forest fire with a 12 m flame length happens, one sensing node can cover an area of about 848 m diameter (corresponds to a sensing area of ~0.56 km^2). In this case, approximately 400 windmill-structured energy harvesters with such temperature switches are desired for the Uwharrie forest which is located in northern California with a total area of 204.95 km^2 [38]. Compared with the enormous loss caused by a serious spread forest fire (which is often up to tens of millions of dollars), the cost of setting up this kind of self-powered intelligent network is insignificant (only several thousands of dollars). Moreover, the most significant issue is that the safety of residents will be guaranteed. The fabricated energy harvester requires 13 s in order to save enough power for emitting an 8-bit data at a distance of 400 m between a wireless sensor and a receiver. Air flow velocity was expected as about 9 m/s in the analysis [39].

4.4. Further improvement in future work

In future work on this design, the windmill structure will be optimized and minimized to meet the requirements of more practical industrial applications while the same level of performance is maintained. Considering the air flow in the forest is very random, a rotating axis is connected to the fixed base and a rudder is integrated at the bottom of a windmill house. These structures help an alignment of wind blades toward unforeseen wind direction. Thus, the proposed energy harvester scavenge more potential wind power source with the rudder coupled with a rotating axis. Structural optimization by adjusting the size of surface structures and the curve angle of the blades can yield higher aerodynamic efficiency. Moreover, the optimization of the frame shape will benefits the minimization of turbulent flow and air mixing around the windmill structure caused by the frame itself. Commercial copper coils with more numbers of turns and less volume can be utilized for size reduction and output enhancing. In addition, a better highly lubricated bearing can be adopted to further reduce the friction and increase the rotating frequency, as well as the output voltage. A material with higher temperature tolerance will be used to manufacture the energy harvester to overcome the temperature issues and expand the application of this design. To further decrease in manufacturing cost and size, MEMS technology could be employed for the fabrication of the miniaturized high-efficient windmill structure [40]. It should be noted that this design can be used for not only scavenging wind energy but also for scavenging fluid flow energy, which may be used in the temperature monitoring of ocean currents for improvement of the environment.

5. Conclusions

In this paper, we have discussed the design, fabrication and evaluation of a unique windmill-structured energy harvester which can perform well in wireless forest fire monitoring application. Various types of blade were designed, simulated and experimentally characterized to identify the blade with the highest aerodynamic efficiency for this windmill-structure. With an input wind velocity in the range from 0 m/s to 18 m/s, the fabricated energy harvester generated a peak voltage of 5.2 V and a peak power of 60 mW with a 150 Ω load resistance. Moreover, at a wind speed of 3 m/s, an average output power of 3 mW was achieved. A wireless transmission module was designed and connected to the energy harvester to demonstrate the performance of this design for the case of a forest fire. The experimental results proved that the windmill-structured energy harvester discussed here can perform well in wireless forest fire monitoring application.

Acknowledgments

This research was supported by National Research Foundation of Korea (NRF) Grant funded by the MEST of the Korean government

(No. 2012K1A3A1A20031500) and International Collaborative R&D Program through KIAT grant funded by the MOTIE (N0000894).

Appendix A. Supplementary data

Supplementary data associated with this article can be found, in the online version, at http://dx.doi.org/10.1016/j.sna.2014.09.002.

References

[1] M. Hefeeda, M. Bagheri, Forest fire modeling and early detection using wireless sensor networks, Ad Hoc Sens. Wirel. Netw. 7 (2009) 169–224.
[2] C. Chandler, P. Cheney, P. Thomas, L. Trabaud, D. Williams, Forest Fire Behavior and Effects in Fire in Forestry, vol. 1, John Wiley & Sons, Inc., 1983, ISBN 978-0-471-87442-3.
[3] Total Wildland Fires and Acres, National Interagency Fire Center, 2014 http://www.nifc.gov/fireInfo/fireInfo_stats_totalFires.html (accessed 26.04.14).
[4] Black Forest Fire. http://en.wikipedia.org/wiki/Black_Forest_Fire (accessed 26.04.14).
[5] P.S. Jadhav, V.U. Deshmukh, Forest fire monitoring system based on Zig-bee wireless sensor network, Int. J. Emerg. Technol. Adv. Eng. 2 (12) (2012) 187–191.
[6] I.F. Akyildiz, Wireless sensor networks: a survey, Comput. Netw. 38 (2002) 393–422.
[7] H. Messer, Environmental monitoring by wireless communication networks, Science 312 (5774) (2006) 713.
[8] P. Constantinou, P.H. Mellor, P.D. Wilcox, A magnetically sprung generator for energy harvesting applications, IEEE/ASME Trans. Mechatron. 17 (3) (2012) 415–424.
[9] S. Roundy, Energy harvesting for tire pressure monitoring systems: design considerations, in: Proceedings of Power MEMS, 2008, pp. 1–6.
[10] Y.M. Zhang, S.B. He, J.M. Chen, Y.X. Sun, X.M. Shen, Distributed sampling rate control for rechargeable sensor nodes with limited battery capacity, IEEE Trans. Wirel. Commun. 12 (6) (2013) 3096–3106.
[11] J. Yang, X.H. Yue, Y.M. Wen, P. Li, Q.M. Yu, X.L. Bai, Design and analysis of a 2D broadband vibration energy harvester for wireless sensors, Sensors Actuat. A-Phys. 205 (1) (2014) 47–52.
[12] X. Wu, M. Parmar, D.W. Lee, A seesaw-structured energy harvester with super-wide bandwidth for TPMS application, IEEE/ASME Trans. Mechatron. 19 (5) (2014) 1514–1522.
[13] R.J.M. Vullers, R.V. Schaijk, I. Doms, C.V. Hoof, R. Mertens, Micropower energy harvesting, Solid State Electron. 53 (2009) 684–693.
[14] C. Alippi, C. Galperti, An adaptive system for optimal solar energy harvesting in wireless sensor network nodes, IEEE Trans. Circuits Syst. I: Regul. Pap. 55 (6) (2008) 1742–1750.
[15] J. Scruggs, P. Jacob, Harvesting ocean wave energy, Science 323 (5918) (2009) 1176–1178.
[16] Q.C. Tang, Y.L. Yang, X.X. Li, Bi-stable frequency up-conversion piezoelectric energy harvester driven by non-contact magnetic repulsion, Smart Mater. Struct. 20 (12) (2011) 1–6.
[17] F. Fei, J.D. Mai, W.J. Li, A wind-flutter energy converter for powering wireless sensors, Sensors Actuat. A-Phys. 173 (1) (2012) 163–171.
[18] A.H. Sodano, J.D. Inman, G. Park, Comparison of piezoelectric energy harvesting devices for recharging batteries, J. Intell. Mater. Syst. Struct. 16 (10) (2005) 799–807.
[19] A. Bibo, M.F. Daqaq, Investigation of concurrent energy harvesting from ambient vibrations and wind using a single piezoelectric generator, Appl. Phys. Lett. 102 (243904) (2013) 1–4.
[20] D.J. Li, S. Hong, S.Y. Gu, Y.Y. Choi, S. Nakhmanson, O. Heinonen, D. Karpeev, K. No, Polymer piezoelectric energy harvesters for low wind speed, Appl. Phys. Lett. 104 (012902) (2014) 1–4.
[21] Y.B. Jeon, R. Sood, J.H. Jeong, S.G. Kim, MEMS power generator with transverse mode thin film PZT, Sensors Actuat. A-Phys. 122 (1) (2005) 16–22.
[22] A. Khaligh, P. Zeng, C. Zheng, Kinetic energy harvesting using piezoelectric and electromagnetic technologies—state of the art, IEEE Trans. Ind. Electron. 57 (3) (2010) 850–860.
[23] Q.C. Tang, Y.L. Yang, X.X. Li, Repulsively driven frequency-increased-generators for durable energy harvesting from ultra-low frequency vibration, Rev. Sci. Instrum. 85 (045004) (2014) 1–5.
[24] T. Galchev, Micro power generator for harvesting low-frequency and nonperiodic vibrations, J. Microelectromech. Syst. 20 (4) (2011) 852–866.
[25] M.J. Schroeder, C.C. Buck, Fire Weather-Chapter 7: Convective Winds. Agriculture Handbook 360, Department of Agriculture, Forest Service, Washington, DC, USA, 1970.
[26] R. Kingman, S.C. Rowland, S. Popescu, An experimental observation of Faraday's law of induction, Am. J. Phys. 70 (6) (2002) 595–598.
[27] D. Saeidi, A. Sedaghat, P. Alamdari, A.A. Alemrajabi, Aerodynamic design and economical evaluation of site specific small vertical axis wind turbines, Appl. Energy 101 (2013) 765–775.
[28] Sauer Energy. http://www.sauerenergy.com/index.php?option=com_content&view=article&id=50&Itemid=60 (accessed 26.04.14).
[29] S. Eriksson, H. Bernhoff, M. Leijon, Evaluation of different turbine concepts for wind power, Renew. Sust. Energy Rev. 12 (2008) 1419–1434.
[30] E. Bassoli, A. Gatto, L. Luliano, M.G. Violentte, 3D printing technique applied to rapid casting, Rapid Prototyp. J. 13 (3) (2007) 148–155.
[31] S. Cullen, Trees and wind: wind scales and speeds, J. Arboric. 28 (5) (2002) 237–242.
[32] E. Sardini, M. Serpelloni, An efficient electromagnetic power harvesting device for low-frequency applications, Sensors Actuat. A-Phys. 172 (2) (2011) 475–482.
[33] R. Elfrink, First autonomous wireless sensor node powered by a vacuum-packaged piezoelectric MEMS energy harvester, IEEE Electron Dev. Meet. 22 (5) (2009) 1–4.
[34] M. Löhndorf, T. Kvisterøy, E. Westby, E. Halvorsen, Evaluation of energy harvesting concept for tire pressure monitoring systems, in: Proceedings of Power MEMS, 2007, pp. 331–334.
[35] A. Frey, J. Seidel, I. Kuehne, System design of a piezoelectric MEMS energy harvesting module based on pulsed mechanical excitation, in: Proceedings of Power MEMS, 2010, pp. 29–32.
[36] N. Wu, H. Ogai, Coordinative platoon running of SEV based on vehicle-to-vehicle communication, in: Proceedings of SICE Annual Conference, 2013, pp. 2676–2681.
[37] J.I. Huircán, C. Munoz, H. Young, L.V. Dossow, J. Bustos, G. Vivallo, M. Toneatti, ZigBee-based wireless sensor network localization for cattle monitoring in grazing fields, Comput. Electron. Agric. 74 (2) (2010) 258–264.
[38] National Forests in North Carolina. U.S. Forest Service (Retrieved 17.10.12).
[39] W.R. Heinzelman, A. Chandrakasan, H. Balakrishnan, Energy-efficient communication protocol for wireless microsensor networks, in: IEEE Hawaii International Conference on Systems Sciences, 2000, pp. 1–10.
[40] T.N. Pornsin-sirirak, Y.C. Tai, H. Nassef, C.M. Ho, Titanium-alloy MEMS wing technology for a micro aerial vehicle application, Sensors Actuat. A-Phys. 89 (1) (2001) 95–103.

Biographies

Xuan Wu received the B.Eng. and M.Eng. degrees in mechanical engineering from Chongqing University of Technology, Chongqing, China, in 2009 and 2012, respectively. He is currently working toward the Ph.D. degree in mechanical engineering in the MEMS and Nanotechnology Laboratory, Department of Mechanical Engineering, Chonnam National University, Korea. He is the holder of two patents in China. He is also a member of the Korean Sensors Society. His current research interests include energy-harvesting technology, MEMS device design and fabrication, piezo-materials for various applications, and graphene local anodic lithography technology.

Dong-Weon Lee received the Ph.D. degrees in Mechatronics engineering from Tohoku University, Sendai, Japan, in 2001. He has been a Professor of Mechanical Systems Engineering at Chonnam National University (CNU), Republic of Korea since March of 2004. Previously, he was with the IBM Zurich Research Laboratory in Switzerland, working mainly on micro cantilever devices for chemical AFM applications. At CNU, his research interests include smart cantilever devices, miniaturized energy harvester, smart materials and structures, and nanoscale transducers. He is a member of the technical program committee of IEEE Sensors Conference, Transducers, and Micro processes and Nanotechnology Conference (MNC).